

RESEARCH ARTICLE

Open Access



The protective role of the 3-mercaptopyruvate sulfurtransferase (3-MST)-hydrogen sulfide (H₂S) pathway against experimental osteoarthritis

Sonia Nasi¹, Driss Ehrichiou¹, Athanasia Chatzianastasiou^{2,3}, Noriyuki Nagahara⁴, Andreas Papapetropoulos^{3,5}, Jessica Bertrand⁶, Giuseppe Cirino⁷, Alexander So¹ and Nathalie Busso^{1*}

Abstract

Background: Osteoarthritis (OA) is characterized by the formation and deposition of calcium-containing crystals in joint tissues, but the underlying mechanisms are poorly understood. The gasotransmitter hydrogen sulfide (H₂S) has been implicated in mineralization but has never been studied in OA. Here, we investigated the role of the H₂S-producing enzyme 3-mercaptopyruvate sulfurtransferase (3-MST) in cartilage calcification and OA development.

Methods: 3-MST expression was analyzed in cartilage from patients with different OA degrees, and in cartilage stimulated with hydroxyapatite (HA) crystals. The modulation of 3-MST expression in vivo was studied in the meniscectomy (MNX) model of murine OA, by comparing sham-operated to MNX knee cartilage. The role of 3-MST was investigated by quantifying joint calcification and cartilage degradation in WT and 3-MST^{-/-} meniscectomized knees. Chondrocyte mineralization in vitro was measured in WT and 3-MST^{-/-} cells. Finally, the effect of oxidative stress on 3-MST expression and chondrocyte mineralization was investigated.

Results: 3-MST expression in human cartilage negatively correlated with calcification and OA severity, and diminished upon HA stimulation. In accordance, cartilage from meniscectomized OA knees revealed decreased 3-MST if compared to sham-operated healthy knees. Moreover, 3-MST^{-/-} mice showed exacerbated joint calcification and OA severity if compared to WT mice. In vitro, genetic or pharmacologic inhibition of 3-MST in chondrocytes resulted in enhanced mineralization and IL-6 secretion. Finally, oxidative stress decreased 3-MST expression and increased chondrocyte mineralization, maybe via induction of pro-mineralizing genes.

Conclusion: 3-MST-generated H₂S protects against joint calcification and experimental OA. Enhancing H₂S production in chondrocytes may represent a potential disease modifier to treat OA.

Keywords: Calcium-containing crystals, Osteoarthritis, Animal model, Hydrogen sulfide, Chondrocyte calcification

* Correspondence: Nathalie.Busso@chuv.ch

¹Service of Rheumatology, Department of Musculoskeletal Medicine, Centre Hospitalier Universitaire Vaudois and University of Lausanne, Lausanne, Switzerland

Full list of author information is available at the end of the article



© The Author(s). 2020 **Open Access** This article is licensed under a Creative Commons Attribution 4.0 International License, which permits use, sharing, adaptation, distribution and reproduction in any medium or format, as long as you give appropriate credit to the original author(s) and the source, provide a link to the Creative Commons licence, and indicate if changes were made. The images or other third party material in this article are included in the article's Creative Commons licence, unless indicated otherwise in a credit line to the material. If material is not included in the article's Creative Commons licence and your intended use is not permitted by statutory regulation or exceeds the permitted use, you will need to obtain permission directly from the copyright holder. To view a copy of this licence, visit <http://creativecommons.org/licenses/by/4.0/>. The Creative Commons Public Domain Dedication waiver (<http://creativecommons.org/publicdomain/zero/1.0/>) applies to the data made available in this article, unless otherwise stated in a credit line to the data.

Background

Osteoarthritis (OA) is the most common joint disease affecting millions of people [1]. It is characterized by cartilage degradation, subchondral bone sclerosis and synovitis [2]. In addition, calcium-containing crystals within joint structures are another prominent features of OA, and they participate in its initiation and progression. These crystals were found in 50% up to 100% of synovial fluid [3] and cartilage [4] from OA patients undergoing joint replacement. Two families of calcium-containing crystals were identified in OA: basic calcium phosphate (BCP) (e.g., hydroxyapatite (HA)), and calcium pyrophosphate dihydrate (CPPD) [5]. In vitro, BCP crystals induced catabolic and inflammatory responses [6, 7]. When injected into mice knees, they caused mild synovitis but severe cartilage damage, resembling human OA features [8]. In our recent study, we observed BCP calcific deposits in joints following meniscectomy. Moreover, we found reciprocal crosstalk between BCP and IL-6 production [9], and a positive correlation between these two entities and the severity of cartilage degradation. Thus, we hypothesize that inhibiting crystal formation and deposition in the joint could be of therapeutic value for OA treatment.

Hydrogen sulfide (H_2S) is an endogenous gasotransmitter in our body, together with nitric oxide (NO) and carbon monoxide (CO) [10]. In mammalian tissues, H_2S is generated by three different enzymes: cystathionine beta-synthase (CBS), cystathionine gamma-lyase (CSE), and 3-mercaptopyruvate sulfurtransferase (3-MST). These enzymes use cysteine as a substrate to produce H_2S [11, 12], and their expression is tissue-specific. H_2S showed biological effects [13] that can be of relevance in OA, such as reduced pro-inflammatory responses [14], reduced mineralization [15–18], improved anabolic/catabolic balance [19, 20], and decreased oxidative stress (reactive oxygen species (ROS) production) [21, 22]. H_2S signaling occurs in part through post-translational modification (namely, S-sulfhydration) of specific cysteine residues in target proteins with the potential to alter their function [23]. In addition, H_2S oxidation leads to sulfite (SO_3^{2-}), thiosulfate ($S_2O_3^{2-}$) [24], and sulfate (SO_4^{2-}) generation in the mitochondria [12], which could themselves mediate H_2S effects.

Current therapeutic approaches for OA are either symptomatic or surgical. Therefore, there is a medical need for interventions that target the pathological processes of OA. We hypothesized that H_2S can prevent calcium-containing crystals deposition in the joint, and subsequently OA progression. In particular, we demonstrated that activation of the 3-MST/ H_2S axis improved outcomes in both human and experimental OA.

Methods

Mice and experimental osteoarthritis

3-MST KO ($n = 8$) [25] and WT female mice ($n = 8$), 8-weeks old, on a C57BL/6 background, were subjected to medial meniscectomy (MNX) of the right knee, while the contralateral knee was sham-operated as control [26]. Two months after, mice were sacrificed, blood collected, and serum obtained by 15 min centrifugation at $15000\times g$, and knees fixed in 10% formalin.

MicroCT-scan

MicroCT-scans analysis was performed using a SkyScan 1076° X-ray μ CT scanning system (SkyScan, Belgium) and the following parameters: 18 μ m resolution, 60 kV, 167 μ A, 0.4° rotation step over 360°, 0.5 mm Aluminum filter, 1180 ms exposure time. Ex vivo samples acquisition was made using formol fixed knees. Images were reconstructed using NRecon Version 1.6.6.0 (Skyscan, Belgium) considering the following parameters: gray-values = 0.0000–0.105867, ring artifact reduction = 3, beam hardening correction = 40% [27]. Newly formed calcific deposits at the site of the removed medial meniscus were considered as Volumes-Of-Interest (VOI) for the quantitative analysis of new formation volume (mm^3) and new formation crystal content (μ g) by CTA-analyzer V.1.10.

Mouse knee histology

Knees were decalcified in EDTA for 20 days and embedded in paraffin. Sagittal sections (5 μ m thick, 3 sections/mouse, spaced 70 μ M apart) of the medial compartment were stained with Safranin-O and counterstained with fast green/iron hematoxylin. Blinded OARSI score (0–24 score) [28] for cartilage damage and Safranin-O loss was assessed by two independent observers.

Thiosulfate measurement

Serum was delipidized with dichloromethane and centrifuged. The supernatant was derivatized with monobromobimane, acetonitrile, and HEPES/EDTA buffer (pH 8) for 30 min in the dark. Methanosulfonic acid was added to stop the reaction and proteins removed by centrifugation. Thiosulfate was determined by HPLC [29, 30]: Waters-2695 module, fluorescence detector (excitation wavelength of 380 nm, the emission wavelength of 480 nm) and a reverse-phase column. The eluants were PIPES (10 mM, pH 6.6) and methanol (gradient). Concentrations were calculated by integrating the area under the curve.

Human cartilage explants

Human cartilage (tibia and femur) from 15 OA patients undergoing knee replacement (Kellgren-Lawrence K/L score 1 to 4, age 64.69 years \pm 10.58) was obtained from

the Otto-von-Guericke University (Magdeburg-D). Patients were grouped into low (K/L 1–2 and OARSI 2–3, age 70.25 ± 5.37 years), medium (K/L 3 and OARSI 3–4, age 65.25 ± 14.88 years), and high (K/L 4 and OARSI 5, age 59.8 ± 9.33 years) OA grade. Full-thickness cartilage explants were fixed in 4%PFA and embedded in paraffin. Five-micrometer-thick sagittal sections were cut for further immunohistochemical and calcification analysis.

For HA crystal stimulation experiment, cartilage (tibia and femur) from 4 OA patients (mean age 72 ± 10 years) undergoing knee replacement (K/L score = 4) was obtained from the Orthopedic Department (CHUV, Lausanne-CH). Six-millimeter-diameter disks (3 disks/patient) were dissected from macroscopically intact cartilage using a dermal punch. In order to match for location across treatment groups, each disk was divided into two equal parts, and each half was stimulated or not with 500 $\mu\text{g}/\text{ml}$ HA crystals for 24 h in DMEM+1%P/S + 50 $\mu\text{g}/\text{ml}$ L-ascorbic acid 2-phosphate. Cartilage was fixed in 4%PFA for immunohistochemical analysis.

Human cartilage histology and quantification of calcification

For each patient, three sections of full-thickness cartilage were stained with Von Kossa/Safranin-Orange staining (Sigma). Pictures were taken using a Zeiss Axiovert microscope and Zen software at $\times 2.5$ magnification, in order to have the whole cartilage section depicted on the picture. Images were then converted into a grayscale. The total cartilage area (100%) was marked in the image using ImageJ (NIH Image). The percentage (%) of calcified cartilage over the total cartilage area was identified using a threshold for black and white. The mean value of the three sections/patient was calculated. Four to 5 patients were analyzed for each K/L-OARSI group.

Immunohistochemical analysis

3-MST expression was evaluated using an anti-3-MST rabbit polyclonal antibody (Novusbio NBP1-82617) on paraffin sections. The antibody was demonstrated to be specific, as a negative staining was obtained both when 3-MST IHC was performed without the primary antibody (data not shown) and when 3-MST IHC was performed on knee sections from 3-MST KO mice (Fig. 2a, Sham 3-MST KO).

Analysis of 3-MST expression in sham-operated versus meniscectomized murine knees was made by evaluation of positivity in histological sections. In humans, for each patient, three sections of full-thickness cartilage were stained with the 3-MST Ab. Pictures of three fields per section were taken using a Zeiss Axiovert microscope and Zen software at $\times 10$ magnification. The total number of cells and the number of 3-MST-positive cells were counted in each field, and the percentage (%) of 3-MST-

positive cells was calculated. The mean value of the three fields was calculated for each section and the mean value of the three sections/patient was calculated. Four to 5 patients were analyzed for each K/L-OARSI group.

Hydroxyapatite crystals and secondary calciprotein particles

Hydroxyapatite crystals (HA) crystals were synthesized, characterized [31], and sonicated for 5 min in sterile PBS prior to experiment. Secondary calciprotein particles (CPP) were synthesized as previously described [15]. Briefly, 10% FBS, 3.5 mM phosphate (2.14 mM Na_2HPO_4 , 1.36 mM NaH_2PO_4 , Sigma), 1 mM calcium (CaCl_2 , Sigma), 1%P/S, and 1%L-Glutamine were added to DMEM. This medium was stored at 37°C for 7 days to generate secondary CPP and then centrifuged at $25000\times g$ for 2 h at 4°C . Calcium content was measured in the resuspended pellet by the QuantiChrom™ Calcium Kit.

Murine articular chondrocytes isolation

Primary knee immature chondrocytes were isolated from 5 to 7 days old mice [9] and amplified for 7 days in DMEM+1%P/S + 10%FBS to reach chondrocytic differentiation [32]. For calcification studies, chondrocytes were cultivated for 24 h in DMEM+1%P/S + 10%FBS, supplemented with secondary calciprotein particles (CPP-50 $\mu\text{g}/\text{ml}$ calcium) to induce calcification and were concomitantly treated with 0.4% DMSO, 500 μM H_2O_2 (Sigma-Aldrich, dissolved in culture medium), 1 mM N-acetylcysteine NAC (Sigma-Aldrich, dissolved in DMSO), or a combination of those. For qRT-PCR studies, separate plates were used and chondrocytes were cultivated for 4 h in DMEM+1%P/S only, supplemented with 0.4% DMSO or 50 μM of the 3-MST inhibitor (compound 3 [33], dissolved in DMSO, kindly provided by Prof. Kenjiro Hanaoka, University of Tokyo). For alkaline phosphatase activity, separate plates were used and chondrocytes were cultivated for 6 h in DMEM+1%P/S only, supplemented with 0.4% DMSO, 50 μM of the 3-MST inhibitor, 500 μM H_2O_2 , or a combination of those.

Crystal detection in articular chondrocyte cultures

For Alizarin Red staining, cells were fixed in 10% formol for 30 min and calcium-containing crystals stained by applying 2% Alizarin red solution (pH 5.3) for 1 h [34]. After washings with tap water, pictures were taken. For calcium content quantification, separate plates were used. Cell monolayers were decalcified with 0.6 M HCl for 24 h. The following day, calcium content was quantified by the QuantiChrom™ Calcium Kit (BioAssay Systems) by reading absorbance at 612 nm using the Spectramax M5e reader (Molecular Devices).

IL-6 quantification in articular chondrocyte cultures

Cell supernatants from the cells used for the measurement of calcium content were assayed using murine IL-6 ELISA kit (eBioscience) and by reading absorbance at 450 nm and 570 nm using the Spectramax M5e reader.

Alkaline phosphatase (Alp) activity in articular chondrocyte cultures

Supernatant was removed, chondrocytes lysed in 0.01% SDS (dissolved in water), and alkaline phosphatase (Alp) activity was measured in cell lysate using a p-Nitrophenyl Phosphate assay (Alpl Assay Kit, Abcam, ab83369) and by reading absorbance at 405 nm.

H₂S detection in articular chondrocyte cultures

Primary murine chondrocytes (10⁶ cells/condition) were treated for 6 h with 50 μM 3-MST inhibitor or 0.4% vehicle (DMSO). They were then resuspended in fluorescence-activated cell sorting (FACS) buffer (5%FCS, 5 mM EDTA in PBS) and the H₂S fluorescent probe P3 added (10 μM, [35]). FACS analysis was performed right after with a UV laser (LSRII SORP cytometer, BD Biosciences) and data processed by FACS Diva (BD Biosciences) and FlowJoX (Tree Star).

LDH measurement in articular chondrocyte cultures

Measurement of the leakage of components from the cytoplasm into the surrounding culture medium has been widely accepted as a valid method to estimate the number of non-viable cells. Lactate dehydrogenase (LDH) in the supernatant was measured using the fluorimetric method CytoTox-ONE™ Homogeneous Membrane Integrity Assay (Promega), by recording fluorescence at an excitation wavelength of 560 nm and an emission wavelength of 590 nm. Culture medium from wells without cells was used as a negative control (0% cytotoxicity), while medium from wells with lysed cells (1% Triton X-100) was used as a positive control (100% cytotoxicity). The percent cytotoxicity of each experimental wells was then calculated as follows: Percent cytotoxicity = [(Experimental value)-(Culture medium value)]/[(Positive control value)-(Culture medium value)] × 100.

ATDC5 chondrogenic cell line

For qRT-PCR analysis, ATDC5 cells (from ATCC cell line) were cultured in DMEM/F12 (1%P/S only) and treated for 4 h with different combinations of 0.4% DMSO (Sigma-Aldrich), 50 μl/ml CPP, 50 μM 3-MST inhibitor, and 500 μM H₂O₂. For reactive oxygen species (ROS) measurement, separate plates were used and ATDC5 were cultured in DMEM/F12 without phenol red and FBS and cells were treated with the same conditions described above, or with 10 ng/ml mouse recombinant IL-6 (Gibco, dissolved in DMSO) where indicated.

ROS level measurement in ATDC5 cells

Mitochondrial ROS level was measured with Red Mitochondrial Superoxide Indicator (MitoSOX, Life Technologies). Briefly, ATDC5 in half area 96-wells clear bottom black plate were stimulated or not for 1 h with 50 μl/ml CPP and treated or not with vehicle 0.4% DMSO, 50 μM 3-MST inhibitor, 50 μM H₂O₂, 1 mM NAC, or 10 ng/ml IL-6 in DMEM/F12 without phenol red. After stimulation, cells were loaded 30 min with 5 μM MitoSOX, and fluorescence intensity measured (excitation wavelength of 510 nm, emission wavelength of 580 nm) using the SpectraX M5e reader.

Wells with cells-DMEM/F12 only, as well as wells with MitoSOX-DMEM/F12 only, were also included in order to measure cells and MitoSOX autofluorescence, respectively. These background values were then subtracted to the experimental wells values, and the obtained results were plotted as MitoSOX signal (A.U).

Real-time PCR analysis in articular chondrocyte cultures and ATDC5 cells

Cells were lysed in TRIzol reagent (Thermo Scientific) in a ratio of 500 μl TRIzol every 10⁶ cells. RNA was extracted (RNA Clean and Concentrator5, Zymoresearch), reverse transcribed (Superscript II, Invitrogen), and quantitative Real Time-PCR (qRT-PCR) with gene-specific primers (Table 1) using the LightCycler480® system (Roche Applied Science) was performed. Each reaction mix was composed by 3.75 μl LightCycler 480 SYBR Green I Master (Roche) + 0.75 μl of 5 μM primer pair specific for each gene + 0.5 μl of LightCycler Water (Roche) + 2.5 μl of 20 ng/μl cDNA. Wells with RNase/DNase-free water instead of cDNA were included for each amplified gene as a negative control.

Table 1 Murine gene specific primers for qRT-PCR

Gene	Forward primer (5' → 3')	Reverse primer (5' → 3')
<i>mAnk</i>	TGT CAA CCT CTT CGT GTC CC	GAC AAA ACA GAG CGT CAG CG
<i>mAlpl</i>	TTG TGC CAG AGA AAG AGA GAG	GTT TCA GGG CAT TTT TCA AGG T
<i>mAnx5</i>	CCT CAC GAC TCT ACG ATG CC	AGC CTG GAA CAA TGC CTG AG
<i>mPit-1</i>	CTC TCC GCT GCT TTC TGG TA	AGA GGT TGA TTC CGA TTG TGC
<i>mPit-2</i>	AAA CGC TAA TGG CTG GGG AA	AAC CAG GAG GCG ACA ATC TT
<i>m3-Mst</i>	CTG GGA AAC GGG GAG CG	GCT CGG AAA AGT TGC GGG
<i>mTbp</i>	CTT GAA ATC ATC CCT GCG AG	CGC TTT CAT TAA ATT CTT GAT GGT C
<i>mGapdh</i>	CTC ATG ACC ACA GTC CAT GC	CAC ATT GGG GGT AGG AAC AC

Data was normalized against *Tbp* and *Gapdh* references genes, with fold induction of transcripts calculated against control cells.

Statistical analysis

For human ex vivo experiments, values represent means \pm SD and 4 to 5 patients per group were analyzed. For in vitro experiments, values represent means \pm SD of triplicates. For each readout, three independent experiments were performed. For in vivo experiments, eight mice per group were used.

Data was analyzed with GraphPad Prism software. The variation between data sets was evaluated using Student's *t* test or one-way or two-way ANOVA test, where appropriate. Bonferroni correction was used as a post hoc analysis in case of multiple comparisons. Correlation between parameters was evaluated using the correlation test and expressed by the Pearson correlation coefficient ($-1 < r < 1$). Differences were considered statistically significant at $*p < 0.05$, $**p < 0.01$, $***p < 0.001$, and $****p < 0.0001$.

Results

3-MST expression in human cartilage negatively correlates with OA severity and chondrocyte calcification, and it is downregulated by HA crystals

Immunohistochemistry on human OA cartilage (Fig. 1a) revealed high 3-MST expression by chondrocytes in the superficial area of cartilage and low expression in intermediate-deep layers. In contrast, chondrocyte calcification was present in deep cartilage and negative in the superficial zone. Thus, we found a trend ($p = 0.08$) towards an inverse correlation ($r = -0.48$) between the two parameters (graph Fig. 1a). When specimens were divided into low, medium, or high OA, 3-MST expression was decreased by 20–30% in medium and high OA (Fig. 1b), while chondrocyte calcification was increased as assessed by von Kossa staining (Fig. 1b). We next stimulated cartilage explants with HA crystals for 24 h (Fig. 1c). 3-MST expression was significantly inhibited by HA crystals in four patients, although at different degrees (Fig. 1c). Altogether, these results indicate that chondrocyte calcification increases during OA progression and negatively impacts on 3-MST expression proportionally to disease severity.

3-MST regulates joint calcification and cartilage damage in experimental OA

To investigate the role of 3-MST in the pathogenesis of osteoarthritis, we subjected 3-MST deficient mice (3-MST KO) to meniscectomy. As in human OA samples, we observed that 3-MST expression was higher in sham-operated healthy knees than in osteoarthritic MNX knees (Fig. 2a). Two months post-surgery, CT-scans

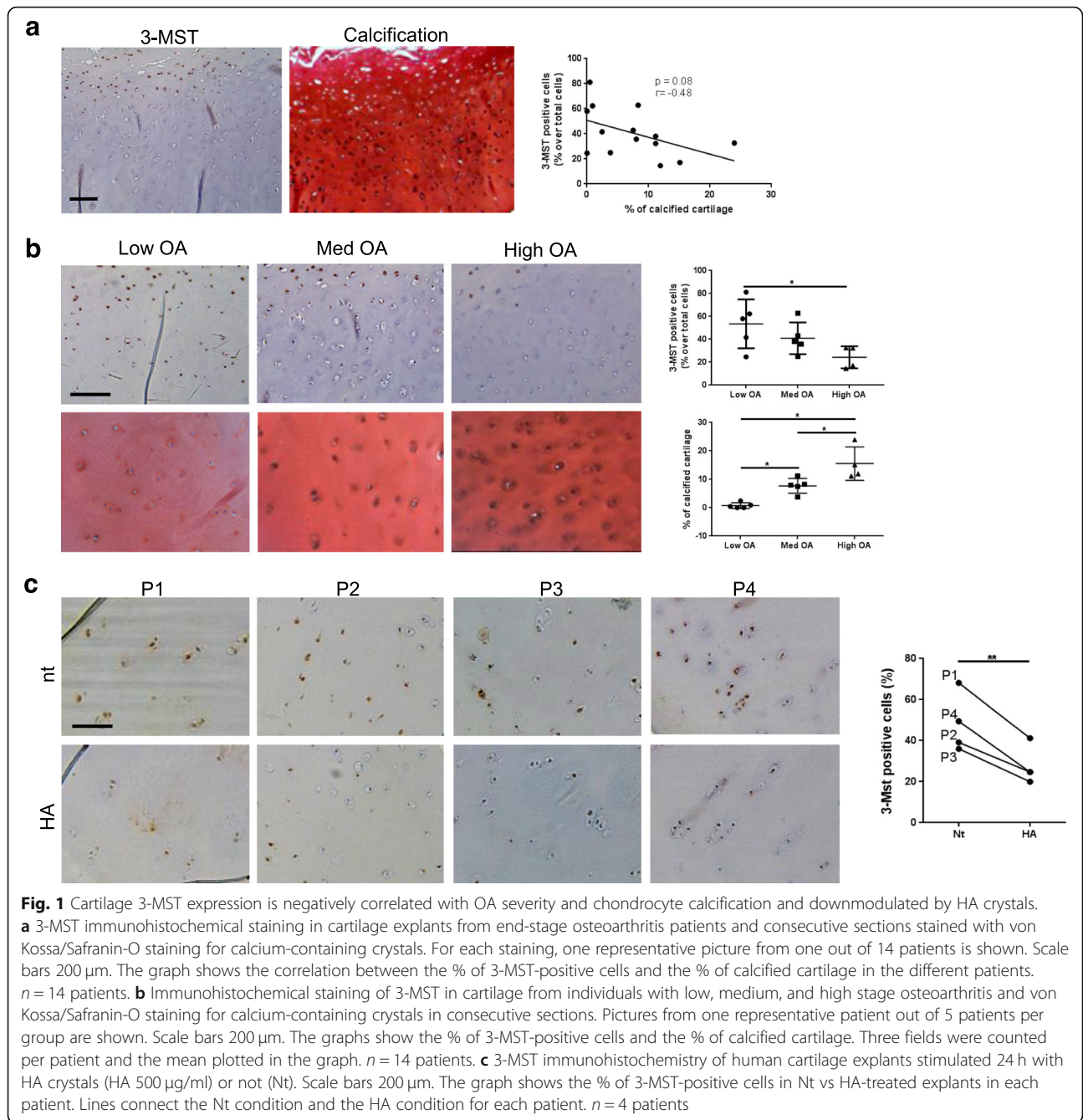
evidenced increased calcification in 3-MST KO knees if compared to WT knees (Fig. 2b, white arrows). Quantitative analysis of calcifications revealed that both their volume and their overall crystal content were significantly higher in 3-MST KO mice (graphs Fig. 2b). In parallel, cartilage damage (fissures and fibrillations, black arrows) as well as proteoglycan loss (reduced Safranin-O staining) were exacerbated in 3-MST KO joints compared to WT joints, as mirrored by both histological analysis and OARSI scores (Fig. 2c). Finally, serum thio-sulfate level was higher in WT mice than in 3-MST KO mice (Fig. 2d).

3-MST regulates chondrocyte mineralization and IL-6 secretion in vitro

After 24 h in the presence of CPP, 3-MST KO chondrocytes had exacerbated mineralization as demonstrated by Alizarin red staining (Fig. 3a) and by quantification of calcium content in the cell monolayer (graph Fig. 3a). In parallel, we found that 3-MST KO cells secreted higher levels of basal IL-6 than WT cells (Fig. 3b). This would support our previous finding that IL-6 sustains mineralization in chondrocytes [9]. As the second approach to lower 3-MST activity, we treated WT chondrocytes with a pharmacological 3-MST inhibitor. Firstly, we confirmed by FACS that the 3-MST inhibitor significantly decreased H_2S production by chondrocytes (Fig. 3c). In accordance with the findings in 3-MST KO chondrocytes (Fig. 3a), treatment with the 3-MST inhibitor triggered chondrocyte mineralization (Fig. 3d). Conversely, stimulation of chondrocytes with crystals (HA or CPP) caused 3-MST downregulation (Fig. 3e). Accordingly, the addition of IL-6 also decreased 3-MST expression by 2-fold (Fig. 3f). Altogether these results suggest that two of the main OA triggers (calcium-containing crystals and IL-6) negatively affect the endogenous generation of H_2S by 3-MST and vice-versa.

Oxidative stress regulates 3-MST expression and mineralization in chondrocytes

Oxidative stress has been implicated in the progression of OA via different mechanisms [36], but never via a direct role in chondrocyte calcification. We found that H_2O_2 stimulation led to significantly decreased 3-MST expression (Fig. 4a) in chondrocyte, but concomitantly increased calcification (Fig. 4b), while the ROS scavenger NAC reverted the latter effect. Cell viability was not affected in any conditions (Fig. 4c). Inversely, neither promoters of calcification (CPP and IL-6) nor H_2S inhibition (3-MST inhibitor) altered mitochondrial ROS production by chondrocytes (Fig. 4d). Taken together, these results support a deleterious role of ROS upstream to chondrocyte calcification and inflammation, likely mediated by inhibition of 3-MST-generated H_2S .

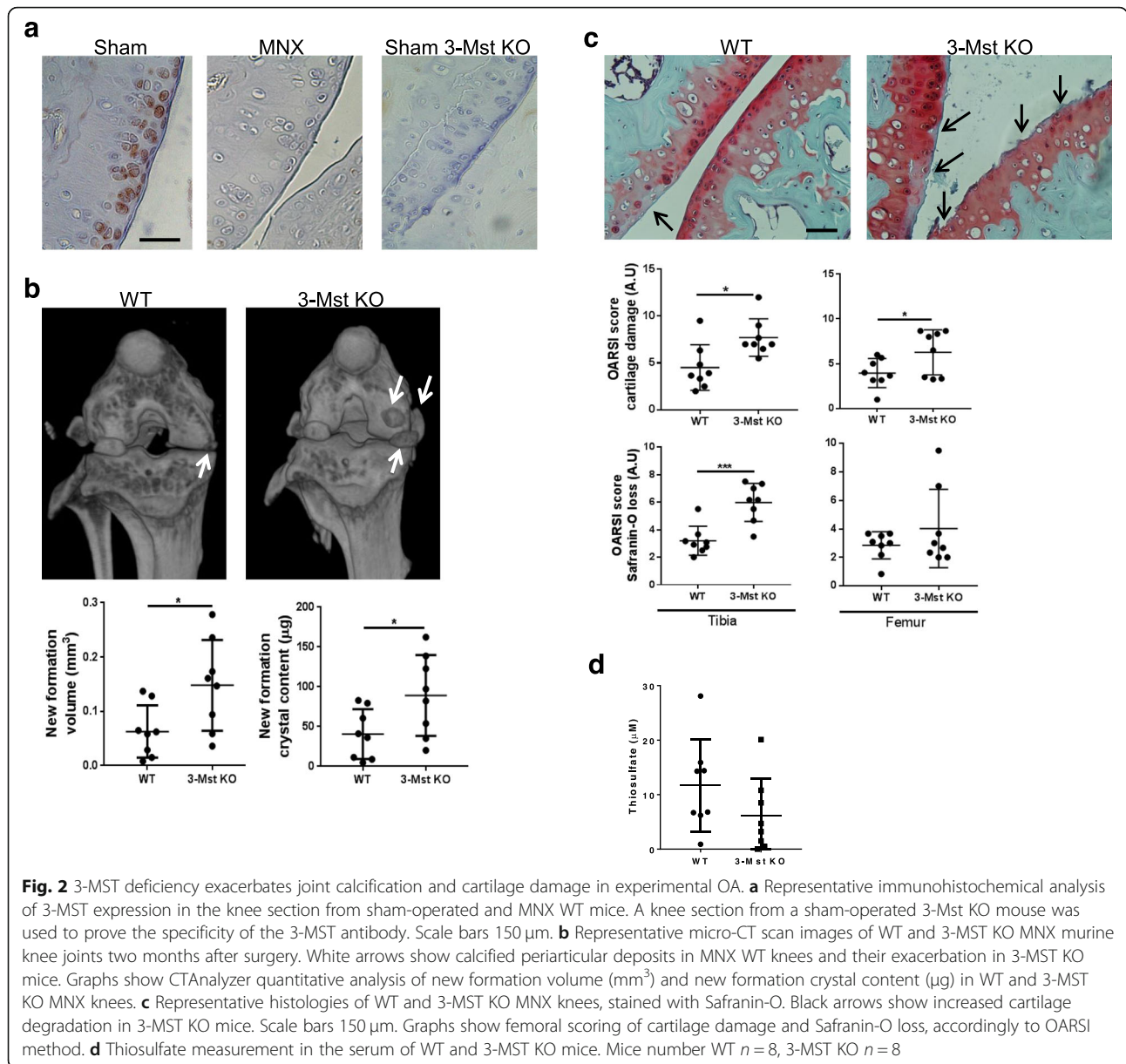


Finally, we assessed the expression of genes involved in the calcification process in chondrocyte cultured in presence of CPP, or H₂O₂, or 3-MST inhibitor. H₂O₂ significantly increased *Ank* and *Anx5* expression, as the pro-calcifying stimulus CPP and the 3-MST inhibitor did (Fig. 4e). This strengthens the hypothesis that H₂O₂ may induce chondrocyte calcification via inhibition of endogenous H₂S production. *Alpl* expression (Fig. 4e) and activity (Fig. 4f), and *Pit1* and *Pit2* expression were not modulated in all conditions.

Discussion

A large body of evidence supports the idea that calcium-containing crystals are active players in the initiation and progression of OA [5, 9, 37, 38]. However, the mechanisms of cartilage calcification are largely unknown and to date, there is no treatment that can prevent crystal deposition or dissolve already formed calcifications.

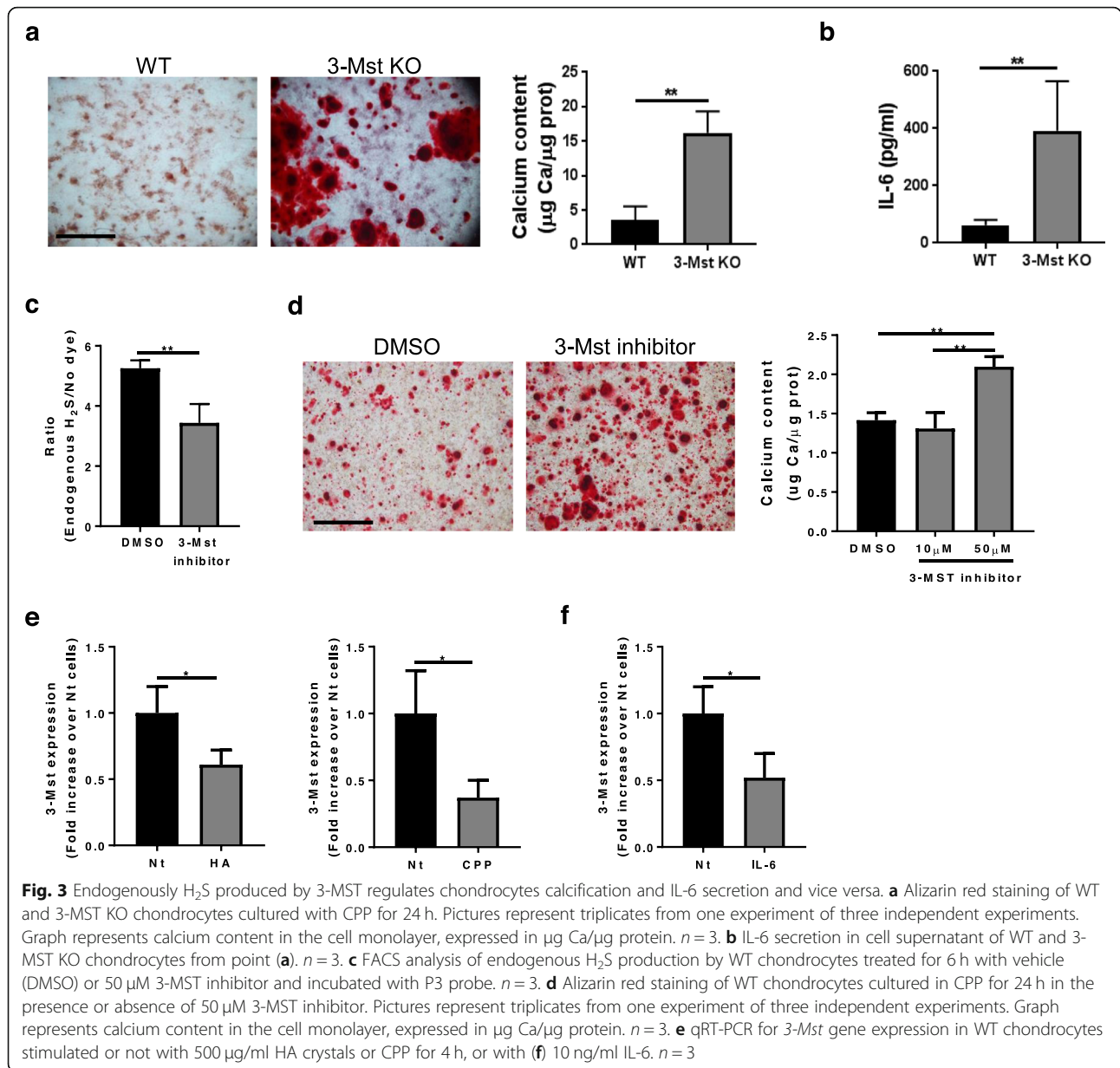
Here, we have demonstrated that the 3-MST/H₂S pathway is involved in cartilage calcification and OA



progression. Decreasing the endogenous level of H_2S in chondrocytes, either genetically by 3-MST deficiency or pharmacologically by an 3-MST inhibitor, led to exacerbated mineralization in vitro (Fig. 3a, d). A proof of concept of the protective role of 3-MST-generated H_2S was given by the in vivo MNX model, where 3-MST-deficient mice were affected by joint calcification and cartilage degradation (Fig. 2b, c) more severely than WT mice. Another evidence was that in knee cartilage from both MNX mice (Fig. 2a) and OA patients (Fig. 1b) we found an inverse correlation between 3-MST expression, and the extent of calcification as well as OA severity.

3-MST deficiency in humans is responsible for a rare inheritable disorder called mercaptolactate-cysteine

disulfiduria (MCDU) [39]. MCDU patients are not only mainly affected by mental retardation [25], but can also exhibit skeletal abnormalities (high forehead, arachnodactyly, genu valgum, and joint hyperflexibility (Orphanet:1035)). Other studies support a protective role of H_2S in pathological mineralization. H_2S decreased vascular calcification [15, 17, 18, 40], while inhibition of CSE activity caused the opposite effect [18]. The H_2S -donor sodium thiosulfate (STS) inhibited knee joint calcification during experimental OA [37]. On the other hand, some studies demonstrated the pro-mineralizing effect of H_2S . H_2S induced physiological mineralization of human periodontal [41] and mesenchymal [42] stem cells. CBS deficiency was associated

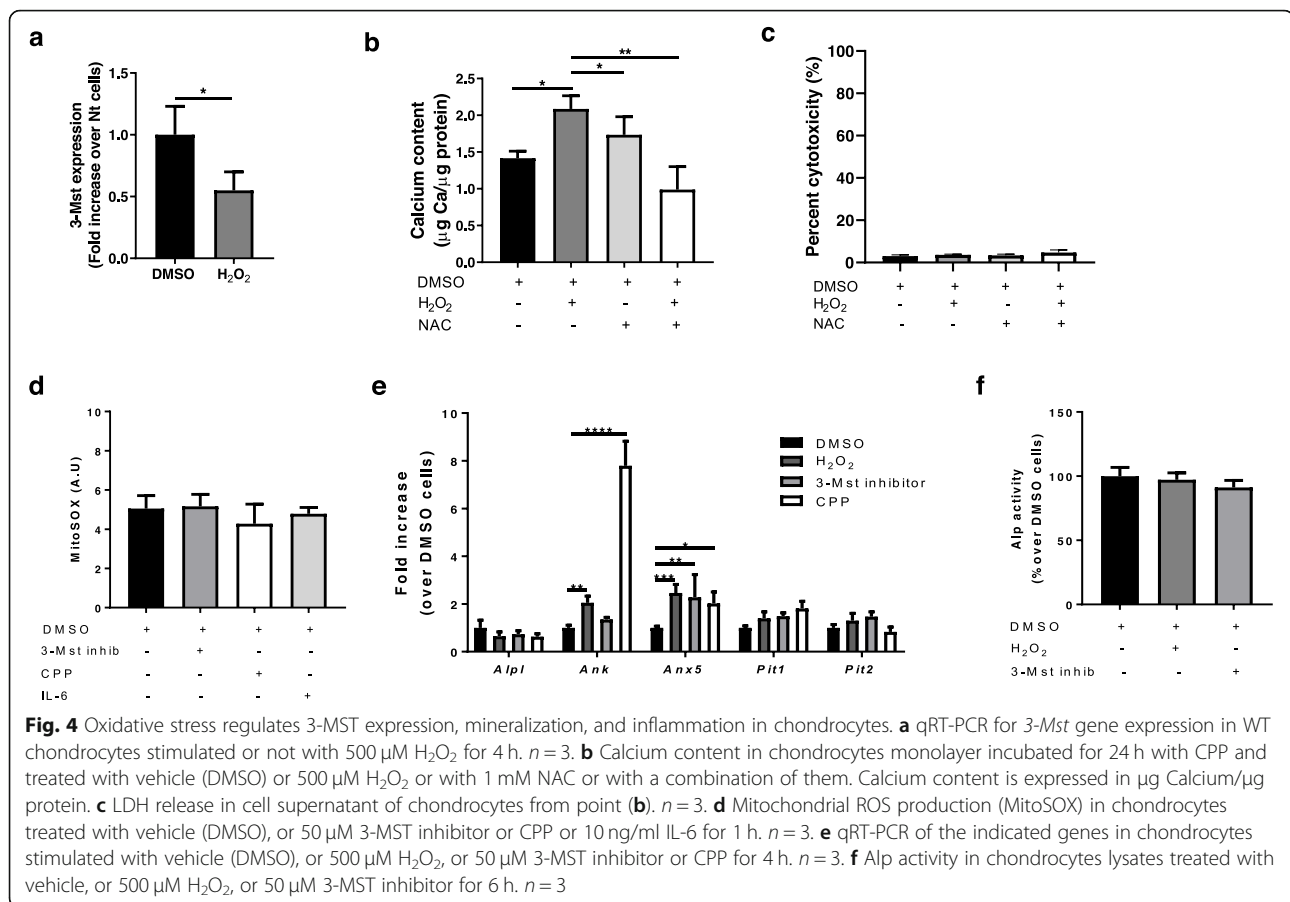


with human [43] and murine [44] osteoporosis. Furthermore, the H₂S-donor GYY4137 stimulated bone formation in vivo [45, 46].

While all these studies investigated the CBS/H₂S or the CSE/H₂S pathway in mineralization, to our knowledge, we are the first to highlight the importance of the 3-MST/H₂S pathway in this context. We will discuss here below the mechanisms by which lack of 3-MST-generated H₂S could facilitate chondrocyte calcification and OA progression and the time-course of the events.

The very first mechanism involved seems to be reduced 3-MST expression/activity by increased oxidative stress. We indeed showed here that hydrogen peroxide (H₂O₂), a major reactive oxygen species (ROS), was able to decrease

3-Mst expression (Fig. 4a). The effect of ORS on 3-MST can also occur at the post-transcriptional level, as it was shown previously that H₂O₂ inhibited the activity of mouse recombinant 3-MST and further H₂S generation [47]. Subsequently to 3-MST inhibition, we showed that H₂O₂ exacerbated chondrocyte mineralization (Fig. 4b) while the ROS scavenger NAC reverted this effect. Other studies exist in the literature that supports an important role of ROS in triggering chondrocyte calcification [48] and metalloproteases production [49, 50], ultimately leading to OA progression. The fact that preventing oxidative stress is beneficial in reducing chondrocyte calcification, was also highlighted in a previous study from our group, in which we demonstrated that the H₂S metabolite

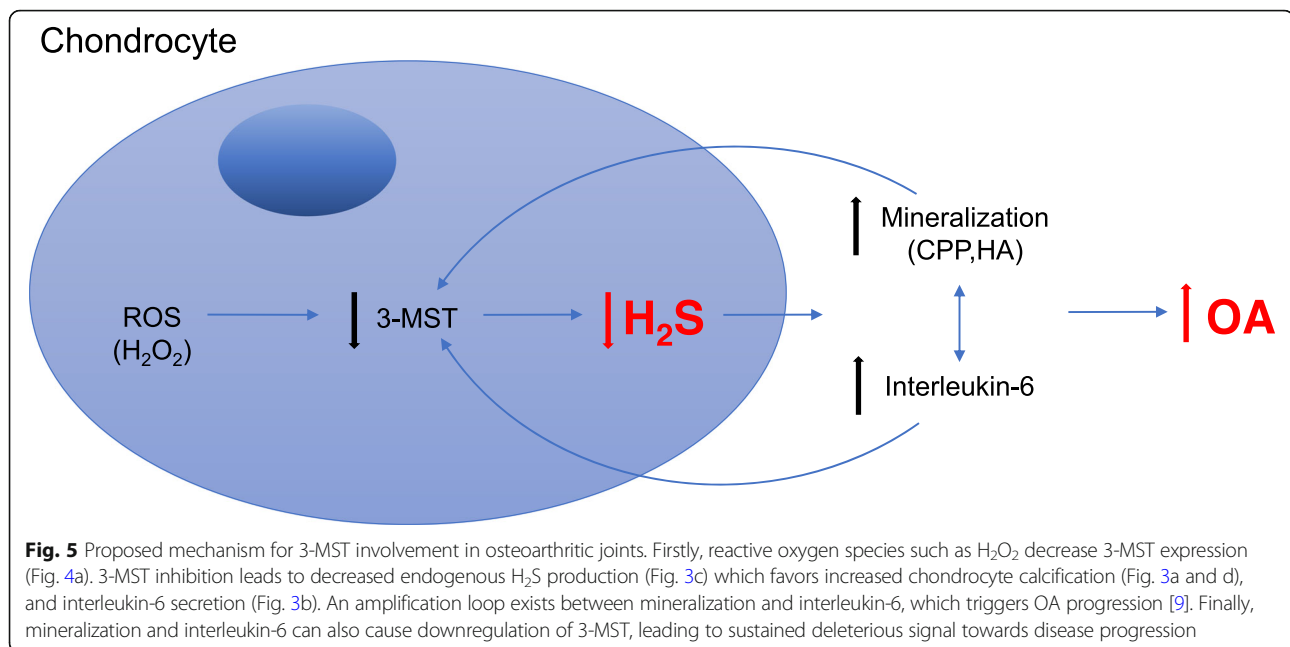


thiosulfate was able to decrease ROS production and calcification in chondrocytes [37]. We therefore hypothesize that increased oxidative stress inhibits 3-MST/ H_2S ultimately leading to increased chondrocyte calcification. Importantly, while ROS suppressed 3-MST/ H_2S pathway and induced calcification, we could not find the opposite, that is 3-MST inhibition or calcification trigger (CPP) did not increase mitochondrial ROS production. This could be because the 3-MST function in mitochondria is compensated by another enzyme called rhodanese [51]. Further investigations are needed to determine if decreased 3-MST/ H_2S impact on total ROS production in chondrocytes.

We next investigated in more details the possible underlying mechanisms by which 3-MST inhibition could exacerbate calcification in chondrocytes, and found that both 3-MST inhibitors (H_2O_2 and the 3-MST inhibitor itself) caused upregulation of calcification genes such as *Ank* and *Anx5* (Fig. 4e). This is in line with our previous data of *Anx5* downregulation by the H_2S metabolite thiosulfate [37]. The expression or the activity of other calcification enzymes and channels (*Alpl*, *Pit1*, *Pit2*) were not impacted by H_2O_2 or the 3-MST inhibitor (Fig. 4e, f).

An additional trigger of chondrocyte calcification is known to be inflammation. In particular, in our study from 2015 [9], we demonstrated that a vicious cycle exists between chondrocyte calcification and the pro-inflammatory cytokine IL-6. In the current study, we demonstrated that 3-MST inhibition (3-MST deficient chondrocytes), led not only to increased calcification but also to increased IL-6 secretion by chondrocytes (Fig. 3b). Conversely, we found that both pro-calcifying factors (HA, CPP) and pro-inflammatory factors (IL-6) led to the downregulation of 3-Mst expression (Fig. 3e, f), thus reducing H_2S . This loop is shown in Fig. 5.

A thing that remains to be clarified is whether the effects caused by inhibition of the 3-MST (exacerbated calcification and inflammation) are due to decreased levels of H_2S or one of its metabolites such as thiosulfate. In 3-MST KO mice, which have decreased serum levels of H_2S [25], we also found decreased serum levels of thiosulfate (Fig. 2b). We previously demonstrated that thiosulfate is protective against joint calcification and cartilage degradation in experimental OA, likely due to its anti-inflammatory, antioxidant, and anti-catabolic properties [37].



Finally, further data are needed to determine whether the other H₂S producing enzymes have a role in calcification in OA. Although we have already excluded a major role for CBS (because not expressed in cartilage, and because we did not observe any OA phenotype in CBS KO mice, data not shown), it is likely that CSE, which is expressed by chondrocytes [52], may as well have a role in joint calcification.

Conclusions

We have established a key role for the 3-MST/H₂S axis in the regulation of pathological chondrocyte calcification in OA. Oxidative stress is an upstream event leading to reduced 3-MST/H₂S levels. Impaired 3-MST/H₂S levels increase chondrocyte calcification and IL-6 secretion. Moreover, calcium-containing crystals and IL-6 can in turn inhibit 3-MST-mediated H₂S production, resulting in even greater mineralization and OA progression (Fig. 5). Whether these phenotypes are due to the lack of H₂S, or the lack of one of its metabolites such as thiosulfate, or the accumulation of the 3-MST substrate 3-mercaptopyruvate remains to be investigated. Our results suggest that augmenting H₂S production by 3-MST activation may be an approach to treat calcifying disorders.

Abbreviation

3-MST: 3-Mercaptosulfur transferase; CBS: Cystathionine beta-synthase; CSE: Cystathionine gamma-lyase; H₂S: Hydrogen sulfide; NO: Nitric oxide; CO: Carbon monoxide; BCP: Basic calcium phosphate; HA: Hydroxyapatite; CPPD: Calcium pyrophosphate dihydrate; CPP: Calciprotein particles; MNX: Meniscectomy; ROS: Reactive oxygen species; NAC: N-acetyl cysteine; VOI: Volume of interests; OARSI: Osteoarthritis research society international; K/L: Kellgren-Lawrence; LDH: Lactate dehydrogenase; Alpl: Alkaline phosphatase; Ank: Progressive ankylosis protein homolog; Anx5: Annexin 5;

Pit1: Phosphate transporter 1; Pit2: Phosphate transporter 2; MCDU: Beta-mercaptolactate cysteine disulfiduria; VSMCs: Vascular smooth muscle cells; IL-6: Interleukin-6

Acknowledgements

We thank Véronique Chobaz for her excellent technical support. We are grateful to Prof. Thomas Hügle for his suggestions, critical reading, and editing of the manuscript. Hydroxyapatite (HA) crystals were kindly provided by Prof. Christèle Combes (CIRIMAT, INPT-UPS-CNRS, Toulouse, France). Serum thiosulfate measurement was kindly performed by Dr. Andreas Pasch (Calcicon AG, Nidau, Switzerland). 3-MST inhibitor was kindly provided by Prof Kenjiro Hanaoka, University of Tokyo.

Authors' contributions

SN designed, performed, and evaluated most experiments. NC took part in the in vivo experiment. NN originally generated the 3-MST knockout mice. AS, AP, GC, and NB designed the project and evaluated results. JB collected and analyzed human cartilage calcification. DE set up and performed FACS analysis. All co-authors participated in the writing of the manuscript. The authors read and approved the final manuscript.

Funding

This work was supported by the Fonds National Suisse de la recherche scientifique (grant 310030-130085/1).

Availability of data and materials

Data are available upon request to authors.

Ethics approval and consent to participate

All animal procedures were in compliance with the European Community guidelines for the use of experimental animals; experimental protocols were approved by the Ethical Committee of the Prefecture of Athens (198177). Animals received a standard rodent laboratory diet. All efforts were made to minimize suffering. Human samples were obtained with the approval of the Centre Hospitalier Universitaire Vaudois ethical committee or by the institutional Review Board of the Faculty of Medicine of the Otto-von-Guericke University (IRB no. 23/16), and written informed consent of patients was obtained.

Consent for publication

Not applicable

Competing interests

The authors declare that they have no competing interests.

Author details

¹Service of Rheumatology, Department of Musculoskeletal Medicine, Centre Hospitalier Universitaire Vaudois and University of Lausanne, Lausanne, Switzerland. ²First Department of Critical Care and Pulmonary Services, Faculty of Medicine, National and Kapodistrian University of Athens, Athens, Greece. ³Laboratory of Pharmacology, Faculty of Pharmacy, University of Athens, Athens, Greece. ⁴Isotope Research Center, Nippon Medical School, Tokyo, Japan. ⁵Center of Clinical, Experimental Surgery & Translational Research, Biomedical Research Foundation of the Academy of Athens, Athens, Greece. ⁶Department of Orthopaedic Surgery, Otto-von-Guericke University, Magdeburg, Germany. ⁷Department of Pharmacy, University of Naples Federico II, Naples, Italy.

Received: 18 October 2019 Accepted: 6 March 2020

Published online: 17 March 2020

References

- Sen R, Hurley JA. Osteoarthritis. In StatPearls. Treasure Island (FL). StatPearls Publishing LLC; 2018. https://eproofing.springer.com/journals_v2/mainpage.php?token=n8ucue4E67lXQzdZsqCJ2CkvZlo62dcyQCptZB5cJmEUCNytt1oWuw.
- Loeser RF, Goldring SR, Scanzello CR, Goldring MB. Osteoarthritis: a disease of the joint as an organ. *Arthritis Rheum*. 2012;64:1697–707.
- Nalbant S, Martinez JA, Kitumnuaypong T, et al. Synovial fluid features and their relations to osteoarthritis severity: new findings from sequential studies. *Osteoarthr Cartil*. 2003;11:50–4.
- Fuerst M, Bertrand J, Lammers L, et al. Calcification of articular cartilage in human osteoarthritis. *Arthritis Rheum*. 2009;60:2694–703.
- Ea HK, Liote F. Advances in understanding calcium-containing crystal disease. *Curr Opin Rheumatol*. 2009;21:150–7.
- Conway R, McCarthy GM. Calcium-containing crystals and osteoarthritis: an unhealthy alliance. *Curr Rheumatol Rep*. 2018;20:13.
- McCarthy GM, Dunne A. Calcium crystal deposition diseases - beyond gout. *Nat Rev Rheumatol*. 2018;14:592–602.
- Easley RA, Patsavas MC, Byrne RH, et al. Spectrophotometric measurement of calcium carbonate saturation states in seawater. *Environ Sci Technol*. 2013;47:1468–77.
- Nasi S, So A, Combes C, et al. Interleukin-6 and chondrocyte mineralisation act in tandem to promote experimental osteoarthritis. *Ann Rheum Dis*. 2016;75:1372–9.
- Polhemus DJ, Lefer DJ. Emergence of hydrogen sulfide as an endogenous gaseous signaling molecule in cardiovascular disease. *Circ Res*. 2014;114:730–7.
- Hughes MN, Centelles MN, Moore KP. Making and working with hydrogen sulfide: the chemistry and generation of hydrogen sulfide in vitro and its measurement in vivo: a review. *Free Radic Biol Med*. 2009;47:1346–53.
- Olson KR. H₂S and polysulfide metabolism: conventional and unconventional pathways. *Biochem Pharmacol*. 2018;149:77–90.
- Rose P, Moore PK, Zhu YZ. H₂S biosynthesis and catabolism: new insights from molecular studies. *Cell Mol Life Sci*. 2017;74:1391–412.
- Gemici B, Wallace JL. Anti-inflammatory and cytoprotective properties of hydrogen sulfide. *Methods Enzymol*. 2015;555:169–93.
- Aghagolzadeh P, Radpour R, Bachtler M, et al. Hydrogen sulfide attenuates calcification of vascular smooth muscle cells via KEAP1/NRF2/NQO1 activation. *Atherosclerosis*. 2017;265:78–86.
- Lin TH, Tang CH, Hung SY, et al. Upregulation of heme oxygenase-1 inhibits the maturation and mineralization of osteoblasts. *J Cell Physiol*. 2010;222:757–68.
- Wu SY, Pan CS, Geng B, et al. Hydrogen sulfide ameliorates vascular calcification induced by vitamin D3 plus nicotine in rats. *Acta Pharmacol Sin*. 2006;27:299–306.
- Zavaczi E, Jeney V, Agarwal A, et al. Hydrogen sulfide inhibits the calcification and osteoblastic differentiation of vascular smooth muscle cells. *Kidney Int*. 2011;80:731–9.
- Burguera EF, Vela-Anero A, Magalhaes J, et al. Effect of hydrogen sulfide sources on inflammation and catabolic markers on interleukin 1 β -stimulated human articular chondrocytes. *Osteoarthr Cartil*. 2014;22:1026–35.
- Vela-Anero A, Hermida-Gomez T, Gato-Calvo L, et al. Long-term effects of hydrogen sulfide on the anabolic-catabolic balance of articular cartilage in vitro. *Nitric Oxide*. 2017;70:42–50.
- Spasov SG, Donus R, Ihle PM, et al. Hydrogen sulfide prevents formation of reactive oxygen species through PI3K/Akt signaling and limits ventilator-induced lung injury. *Oxidative Med Cell Longev*. 2017;2017:3715037.
- Zheng D, Dong S, Li T, et al. Exogenous hydrogen sulfide attenuates cardiac fibrosis through reactive oxygen species signal pathways in experimental diabetes mellitus models. *Cell Physiol Biochem*. 2015;36:917–29.
- Zhang D, Du J, Tang C, et al. H₂S-induced Sulfhydrylation: biological function and detection methodology. *Front Pharmacol*. 2017;8:608.
- Marutani E, Yamada M, Ida T, et al. Thiosulfate Mediates Cytoprotective Effects of Hydrogen Sulfide Against Neuronal Ischemia. *J Am Heart Assoc*. 2015;4(11):1–11.
- Nagahara N, Nagano M, Ito T, et al. Antioxidant enzyme, 3-mercaptopyruvate sulfurtransferase-knockout mice exhibit increased anxiety-like behaviors: a model for human mercaptolactate-cysteine disulfiduria. *Sci Rep*. 2013;3:1986.
- Kamekura S, Hoshi K, Shimoaka T, et al. Osteoarthritis development in novel experimental mouse models induced by knee joint instability. *Osteoarthr Cartil*. 2005;13:632–41.
- Nasi S, So A, Combes C, et al. Interleukin-6 and chondrocyte mineralisation act in tandem to promote experimental osteoarthritis. *Ann Rheum Dis*. 2015;75(7):1372–9.
- Pritzker KP, Gay S, Jimenez SA, et al. Osteoarthritis cartilage histopathology: grading and staging. *Osteoarthr Cartil*. 2006;14:13–29.
- Farese S, Stauffer E, Kalicki R, et al. Sodium thiosulfate pharmacokinetics in hemodialysis patients and healthy volunteers. *Clin J Am Soc Nephrol*. 2011;6:1447–55.
- Newton GL, Dorian R, Fahey RC. Analysis of biological thiols: derivatization with monobromobimane and separation by reverse-phase high-performance liquid chromatography. *Anal Biochem*. 1981;114:383–7.
- Prudhommeaux F, Schiltz C, Liote F, et al. Variation in the inflammatory properties of basic calcium phosphate crystals according to crystal type. *Arthritis Rheum*. 1996;39:1319–26.
- Gosset M, Berenbaum F, Thirion S, Jacques C. Primary culture and phenotyping of murine chondrocytes. *Nat Protoc*. 2008;3:1253–60.
- Hanaoka K, Sasakura K, Suwanai Y, et al. Discovery and mechanistic characterization of selective inhibitors of H₂S-producing enzyme: 3-Mercaptopyruvate Sulfurtransferase (3MST) targeting active-site cysteine. *Sci Rep*. 2017;7:40227.
- Gregory CA, Gunn WG, Peister A, Prockop DJ. An alizarin red-based assay of mineralization by adherent cells in culture: comparison with cetylpyridinium chloride extraction. *Anal Biochem*. 2004;329:77–84.
- Singha S, Kim D, Moon H, et al. Toward a selective, sensitive, fast-responsive, and biocompatible two-photon probe for hydrogen sulfide in live cells. *Anal Chem*. 2015;87:1188–95.
- Lepetsos P, Papavassiliou AG. ROS/oxidative stress signaling in osteoarthritis. *Biochim Biophys Acta*. 1862;2016:576–91.
- Nasi S, Ea HK, Liote F, et al. Sodium thiosulfate prevents chondrocyte mineralization and reduces the severity of murine osteoarthritis. *PLoS One*. 2016;11:e0158196.
- Stack J, McCarthy G. Basic calcium phosphate crystals and osteoarthritis pathogenesis: novel pathways and potential targets. *Curr Opin Rheumatol*. 2016;28:122–6.
- Billaut-Laden I, Rat E, Allorge D, et al. Evidence for a functional genetic polymorphism of the human mercaptopyruvate sulfurtransferase (MPST), a cyanide detoxification enzyme. *Toxicol Lett*. 2006;165:101–11.
- Pasch A, Schaffner T, Huynh-Do U, et al. Sodium thiosulfate prevents vascular calcifications in uremic rats. *Kidney Int*. 2008;74:1444–53.
- Su Y, Liu D, Liu Y, et al. Physiological levels of endogenous hydrogen sulfide maintain the proliferation and differentiation capacity of periodontal ligament stem cells. *J Periodontol*. 2015;86:1276–86.
- Liu Y, Yang R, Liu X, et al. Hydrogen sulfide maintains mesenchymal stem cell function and bone homeostasis via regulation of Ca (2+) channel sulfhydrylation. *Cell Stem Cell*. 2014;15:66–78.
- Levasseur R. Bone tissue and hyperhomocysteinemia. *Joint Bone Spine*. 2009;76:234–40.
- Robert K, Maurin N, Vayssettes C, et al. Cystathionine beta synthase deficiency affects mouse endochondral ossification. *Anat Rec A Discov Mol Cell Evol Biol*. 2005;282:1–7.
- Grassi F, Tyagi AM, Calvert JW, et al. Hydrogen sulfide is a novel regulator of bone formation implicated in the bone loss induced by estrogen deficiency. *J Bone Miner Res*. 2016;31:949–63.

46. Jiang X, Chen Y, Lu K, et al. GYY4137 promotes bone formation in a rabbit distraction osteogenesis model: a preliminary report. *J Oral Maxillofac Surg.* 2015;73:732 e731–6.
47. Modis K, Asimakopoulou A, Coletta C, et al. Oxidative stress suppresses the cellular bioenergetic effect of the 3-mercaptopyruvate sulfurtransferase/hydrogen sulfide pathway. *Biochem Biophys Res Commun.* 2013;433:401–7.
48. Morita K, Miyamoto T, Fujita N, et al. Reactive oxygen species induce chondrocyte hypertrophy in endochondral ossification. *J Exp Med.* 2007;204:1613–23.
49. Reed KN, Wilson G, Pearsall A, Grishko VI. The role of mitochondrial reactive oxygen species in cartilage matrix destruction. *Mol Cell Biochem.* 2014;397:195–201.
50. Del Carlo M, Schwartz D, Erickson EA, Loeser RF. Endogenous production of reactive oxygen species is required for stimulation of human articular chondrocyte matrix metalloproteinase production by fibronectin fragments. *Free Radic Biol Med.* 2007;42:1350–8.
51. Nagahara N, Tanaka M, Tanaka Y, Ito T. Novel Characterization of Antioxidant Enzyme, 3-Mercaptopyruvate Sulfurtransferase-Knockout Mice: Overexpression of the Evolutionarily-Related Enzyme Rhodanese. *Antioxidants (Basel).* 2019;8(5):116–225.
52. Fox B, Schantz JT, Haigh R, et al. Inducible hydrogen sulfide synthesis in chondrocytes and mesenchymal progenitor cells: is H₂S a novel cytoprotective mediator in the inflamed joint? *J Cell Mol Med.* 2012;16:896–910.

Publisher's Note

Springer Nature remains neutral with regard to jurisdictional claims in published maps and institutional affiliations.

Ready to submit your research? Choose BMC and benefit from:

- fast, convenient online submission
- thorough peer review by experienced researchers in your field
- rapid publication on acceptance
- support for research data, including large and complex data types
- gold Open Access which fosters wider collaboration and increased citations
- maximum visibility for your research: over 100M website views per year

At BMC, research is always in progress.

Learn more biomedcentral.com/submissions

